4-15-2011

Optimization of the nanolens consisting of coupled metal nanoparticles: An analytical approach

Greg Sun
University of Massachusetts Boston, greg.sun@umb.edu

Jacob B. Khurgin
Johns Hopkins University

Optimization of the nanolens consisting of coupled metal nanoparticles: An analytical approach

G. Sun and J. B. Khurgin

Related Articles

Comment on "Tunable terahertz-mirror and multi-channel terahertz-filter based on one-dimensional photonic crystals containing semiconductors" [J. Appl. Phys. 110, 073111 (2011)]
J. Appl. Phys. 111, 066105 (2012)

Response to "Comment on 'Tunable terahertz-mirror and multi-channel terahertz-filter based on one-dimensional photonic crystals containing semiconductors'" [J. Appl. Phys. 110, 073111 (2011)]
J. Appl. Phys. 111, 066106 (2012)

Time dependent changes in extreme ultraviolet reflectivity of Ru mirrors from electron-induced surface chemistry
J. Appl. Phys. 111, 063518 (2012)

Fabrication of bioinspired omnidirectional and gapless microlens array for wide field-of-view detections
Appl. Phys. Lett. 100, 133701 (2012)

A combined Kirkpatrick-Baez mirror and multilayer lens for sub-10 nm x-ray focusing
AIP Advances 2, 012175 (2012)

Additional information on Appl. Phys. Lett.

Optimization of the nanolens consisting of coupled metal nanoparticles: An analytical approach

G. Sun[1,a)] and J. B. Khurgin[2]

[1]*Department of Physics, University of Massachusetts Boston, Boston, Massachusetts 02125, USA*
[2]*Department of Electrical and Computer Engineering, Johns Hopkins University, Baltimore, Maryland 21218, USA*

Using a simple and intuitive analytical approach, we perform optimization of a nanolens composed of coupled metal nanoparticles capable of subwavelength focusing of light inside the narrow gap separating the particles. Specifically, we optimize the structure of two nanospheres of different sizes to achieve maximum field enhancement at an off-center position in the gap. We demonstrate that the nanolens of two or more spheres acts simultaneously as an efficient antenna with large dipole and an efficient cavity with small effective volume. © *2011 American Institute of Physics.* [doi:10.1063/1.3581886]

The phenomenon of strong electric field induced by the surface plasmons (SPs) has already found important practical applications in improving sensitivity of Raman or fluorescence measurements[1,2] with progress being made toward other promising applications.[3,4] It is also well understood that a single metal nanoparticle having a simple smooth shape (sphere, ellipsoid, or nanorod) usually provides the electric field enhancement no larger than a Q-factor of the metal,[5,6] which is less than a factor of 10–20 for gold in the visible and near IR. Yet a far more significant enhancement can occur in the intricately structured ensembles of nanoparticles where the field gradually couples from the larger particles serving as antennae into the smaller regions acting as field-concentrating "hot spots."[7–11] Analysis of the complex nanostructures typically involves complex and time consuming numerical procedures[7,8,12] in which the actual physics of enhancement tends to be obscured. Recently we have developed an analytical model for complex metal nanostructures based on eigenmode coupling, which adequately and transparently explains the origin of the enhancement and allows fast optimization.[13] In this letter, we demonstrate the versatility and convenience of our model by performing optimization of a nanolens structure[8] in which the large metal sphere acts as an antenna, allowing the efficient in-coupling of external excitation into the system, where energy gets subsequently transferred into the small sphere acting as a resonator.

It has been established that a single metal nanosphere with a radius of a supports multiple-order SP modes, each with its own resonance frequency $\omega_l = \omega_p \sqrt{l/[l+(l+1)\varepsilon_D]}$, where the mode index $l = 1, 2, \ldots, \infty$ and ω_p is the metal plasmon frequency.[14] It ranges from $\hbar\omega_1 = 1.967$ eV to $\hbar\omega_\infty = 2.261$ eV for Au nanosphere embedded in GaN ($\varepsilon_D = 5.8$). Energy in the lth mode $U_l^{(i)}$ is confined in the effective mode volume $V_{eff,l} = 4\pi a^3/(l+1)^2\varepsilon_D$,[13,15] which is always somewhat less than the volume of the nanosphere itself and decreases rapidly for higher order modes. The surface charge distributions associated with the SP modes are such that the dipole moment vanishes for all higher order modes ($l \geq 2$),

except the $l=1$ mode. This dipole mode is the only one that couples to the external fields for as long as the nanosphere diameter is much smaller than the wavelength while all higher order modes remain uncoupled to external radiation modes. As a result, this dipole mode decays radiatively at a rate proportional to the sphere volume, $\gamma_{rad} = (2\omega/3\varepsilon_D)\chi^3$,[13] where $\chi = (2\pi a/\lambda_D)$ is the metal sphere radius normalized to the wavelength λ_D in the dielectric corresponding to the excitation frequency ω. At the same time, all the modes also experience nonradiative decay due to the imaginary part of the metal dielectric function at roughly the same rate equal to the scattering rate in the metal, $\gamma_{nrad,l} \approx \gamma$.

We shall evaluate the field enhancement by comparing to the electric field E_{foc} in the focal spot of a Gaussian beam in the absence of metal as shown in Fig. 1(a). In case of the Gaussian beam being tightly focused onto a diffraction limited spot of radius $w = \lambda_D/\pi\theta_a$, E_{foc} is related to the incident power $|s_+|^2 = (\sqrt{\varepsilon_D}/Z_0)\pi(w/2)^2 E_{foc}^2$, where Z_0 is the impedance of free space.[16–18] With coupled metal spheres placed at the focal spot, the incident light gets coupled into the dipole modes ($l=1$) of both spheres with an in-coupling coefficient $\kappa_{in} \approx (\theta_a/2)\sqrt{3\gamma_{rad}/2}$.[16–18] Figure 1(b) illustrates the flow of

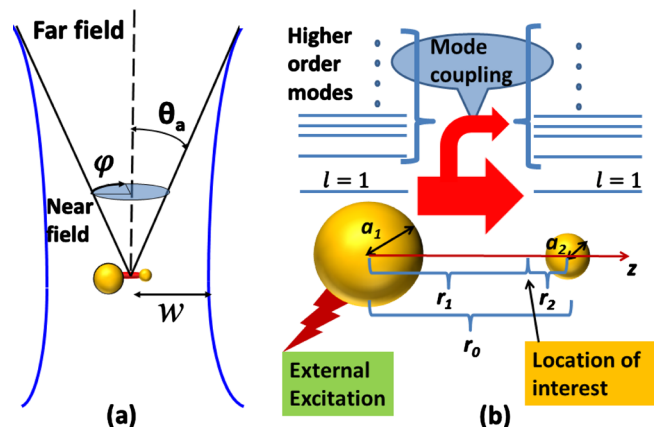FIG. 1. (Color online) Illustration of (a) two coupled metal nanospheres placed at the apex of a focused Gaussian beam with a numerical aperture characterized by the far-field half angle θ_a, and (b) the in-coupling of optical excitation into the dipole mode of the large sphere 1 and their subsequent coupling into all SP modes of the smaller sphere 2.

a)Electronic mail: greg.sun@umb.edu.

98, 153115-1

energy in the nanolens. External excitation couples into the structure primarily via the dipole mode of the large sphere 1, which acts as an antenna because of its large dipole moment. This energy is subsequently transferred to all modes of the small sphere 2 acting as resonators because of their small effective mode volumes. This sequence can be described by a set of rate equations for the mode amplitudes $A_l^{(i)} = \sqrt{U_l^{(i)}}$ of sphere i for its dipole ($l=1$) and higher orders ($l \geq 2$) modes separately as,

$$\frac{dA_1^{(i)}}{dt} = j(\omega_1 - \omega)A_1^{(i)} - \frac{1}{2}(\gamma_{rad}^{(i)} + \gamma)A_1^{(i)} - \frac{1}{2}\sqrt{\gamma_{rad}^{(i)}\gamma_{rad}^{(j)}}A_1^{(j)}$$

$$- j\sum_{l=1}^{\infty} \omega_{1i}\kappa_{1l}^{(ij)}A_l^{(j)} + \kappa_{in}^{(i)}s_+$$

$$\frac{dA_l^{(i)}}{dt} = j(\omega_l - \omega)A_l^{(i)} - j\omega_{1l}\kappa_{1l}^{(ji)}A_1^{(j)} - \frac{\gamma}{2}A_l^{(i)}, \quad l \geq 2, \quad (1)$$

where $\omega_{1l} = \sqrt{\omega_1 \omega_l}$. Included in Eq. (1) are the usual detuning and decay terms for all SP modes, augmented by the super-radiance term $(1/2)\sqrt{\gamma_{rad}^{(i)}\gamma_{rad}^{(j)}}A_1^{(j)}$ that accounts for the coherent character of emission by two dipoles, as well as the coupling between the SP modes of the two spheres described by the coupling coefficient $\kappa_{1l}^{(ij)} = [(l+1)/2](a_i/r_0)^{3/2}(a_j/r_0)^{l+1/2}$.[13]

From steady-state solution of Eq. (1), the field enhancement at a location in the gap of two coupled spheres [Fig. 1(b)] relative to the field in the focal spot E_{foc} in the absence of the metal spheres can be obtained as[13]

$$F = \left| \frac{E(r_1)}{E_{foc}} \right| = \frac{\omega}{\sqrt{2}|M_{2\times2}|} \times \left| (m_{22} - m_{12})\left(\frac{a_1}{r_1}\right)^3 \left[1 \right. \right.$$

$$+ \frac{1}{4}\frac{a_2 r_1^3}{r_0^2 r_2^2}\sum_{l=2}^{\infty}\frac{\omega_{1l}(l+1)^2}{(\omega_l - \omega) + j\frac{\gamma}{2}}\left(\frac{a_2^2}{r_0 r_2}\right)^l \right] + (m_{11} - m_{21})$$

$$\times \left(\frac{a_2}{r_2}\right)^3 \left.\left[1 + \frac{1}{4}\frac{a_1 r_2^3}{r_0^2 r_1^2}\sum_{l=2}^{\infty}\frac{\omega_{1l}(l+1)^2}{(\omega_l - \omega) + j\frac{\gamma}{2}}\left(\frac{a_1^2}{r_0 r_1}\right)^l \right]\right|, \quad (2)$$

where the elements in the 2×2 matrix $M_{2\times2}$ are obtained from the coefficients in Eq. (1)

$$m_{11} = j(\omega - \omega_1) + \sum_{l=2}^{\infty}\frac{\omega_{1l}^2[\kappa_{1l}^{(12)}]^2}{j(\omega - \omega_l) + \frac{\gamma}{2}} + \frac{1}{2}\gamma_1^{(1)},$$

$$m_{12} = \frac{1}{2}\gamma_{rad}^{(2)} + j\omega_1\left(\frac{a_2}{r_0}\right)^3 \quad m_{21} = \frac{1}{2}\gamma_{rad}^{(1)} + j\omega_1\left(\frac{a_1}{r_0}\right)^3,$$

$$m_{22} = j(\omega - \omega_1) + \sum_{l=2}^{\infty}\frac{\omega_{1l}^2[\kappa_{1l}^{(21)}]^2}{j(\omega - \omega_l) + \frac{\gamma}{2}} + \frac{1}{2}\gamma_1^{(2)}. \quad (3)$$

Note the presence of different phases contained in $|M_{2\times2}|$ that appears the denominator of Eq. (2)—this is the direct consequence of delay associated with the energy transfer from one nanoparticle to another, i.e., the retardation effect.
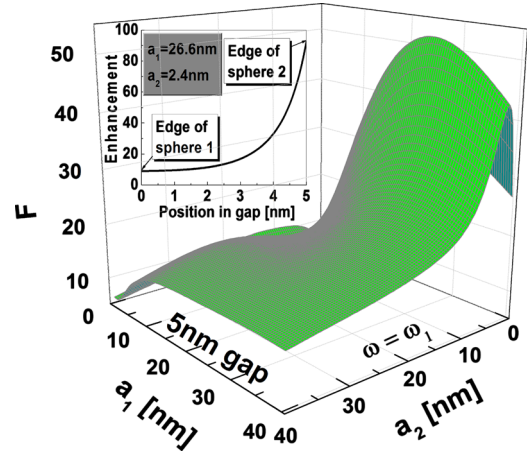

FIG. 2. (Color online) Field enhancement obtained at the frequency of dipole mode, $\omega = \omega_1$, at the location of 0.5 nm from sphere 2 vs the sphere radii a_1 and a_2 that are separated by a 5 nm gap. Inset: the position-dependence of field enhancement from the edge of sphere 1 to sphere 2 at optimized sphere radii $a_1 = 26.6$ nm, $a_2 = 2.4$ nm.

The field enhancement calculated using Eq. (2) at an off-center location, $r_2 - a_2 = 0.5$ nm from the surface of sphere 2 in the 5 nm gap is shown in Fig. 2, when excited at the frequency in resonance with the dipole mode $\omega = \omega_1$. It can be seen that the strongest enhancement is obtained for the two spheres of significantly different dimensions ($a_1 = 26.6$ nm, $a_2 = 2.4$ nm), allowing energy to be coupled in through the large antenna (sphere 1) and then transferred to the small resonator (sphere 2) around which the spot of interest is located. The position-dependence of the enhancement along the 5 nm gap for the same two spheres (inset of Fig. 2) clearly demonstrates that the field is indeed concentrated near the smaller sphere 2 and reaches maximum at its edge.

A full picture of the optimization space can be seen in Fig. 3(a), which shows optimized enhancement at the fixed location of 0.5 nm from sphere 2 as the gap varies from 1 to 30 nm, along with the optimal sphere sizes (a_1, a_2). It can be seen that better enhancement is obtained at smaller gaps, where the coupling between the two spheres is stronger. It is elucidating to see which mode contributes the most to the enhancement, hence in the inset of Fig. 3(a) the ratio of mode energies of sphere 2 to that of the dipole mode of sphere 1, $U_l^{(2)}/U_1^{(1)}$ is plotted for four lowest modes, $l = 1, \ldots, 4$. The mode energy decreases by roughly two orders of magnitude from one mode to the next while the effective volume of the next mode is only a few times smaller, therefore peak fields of higher order modes ($l \geq 2$) are much weaker than the peak field of the dipole mode ($l=1$), and for all practical purposes one can adequately estimate the enhancement using just a two-dipole-mode model. Even though the energy in the dipole mode of the smaller sphere $U_1^{(2)}$ is only a few percent of the dipole mode energy in the larger sphere $U_1^{(1)}$, that energy is contained in a much smaller volume, hence the peak field associated with sphere 2 still exceeds that of sphere 1 by a considerable factor $E_{max,1}^{(2)}/E_{max,1}^{(1)} = (a_1/a_2)^{3/2}(U_1^{(2)}/U_1^{(1)})^{1/2} \geq 10$. A rather simple analytic expression for the field enhancement at the edge of sphere 2, $r_2 = a_2$, is obtained by ignoring all the higher order modes as well as the dipole mode of sphere 1 as $F_{max} \approx \sqrt{2}Q[1 + 4Q^2(a_1/r_0)^6]^{1/2} \approx 2\sqrt{2}Q^2(a_1/r_0)^3$, where the
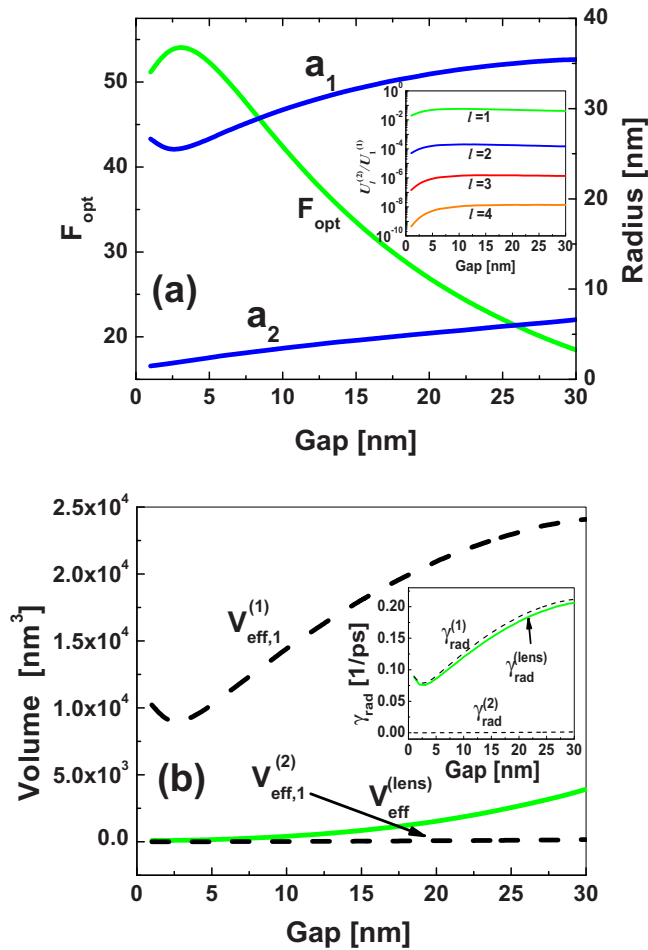
FIG. 3. (Color online) (a) Maximum field enhancement F_{opt} obtained at the frequency of dipole mode, $\omega = \omega_1$ with the optimal Au sphere sizes (a_1, a_2) embedded in the GaN dielectric at the location of 0.5 nm from sphere 2 in a range of gaps that separate the two spheres. Inset: ratio of mode energy of sphere 2 $(l = 1, \ldots, 4)$ to that of the dipole mode of sphere 1, $U_l^{(2)}/U_1^{(1)}$. (b) Effective volume V_{eff}^{Lens} and radiative decay rate γ_{rad}^{Lens} (inset) of the nanolens system compared to those of the dipole mode of both spheres with their optimal sizes.

Q-factor $Q = \omega / \gamma$ (≈ 10 for Au). In the limit of zero gap and the "extreme" nanolens with $a_1 \gg a_2$, $r_0 \approx a_1$, and $F_{max} \approx 2\sqrt{2} Q^2 \approx 300$. This is obviously an overestimate but can be used conveniently as an upper limit of the nanolens enhancement. In comparison to the field enhancement by a single sphere that is proportional to Q, we now have an additional Q-factor for two coupled spheres.

Let us now consider the physical reason for this additional enhancement because revealing this reason may facilitate the design of even more complex structures. As we have noted in our prior letter,[13] the optimal SP structure should on one hand, offer efficient confinement (i.e., should have small effective mode volume), and on the other hand, be efficiently coupled to the free space (i.e., should have large radiative decay rate). Obviously with a single nanoparticle these two demands are irreconcilable but with two (and more) nanoparticles these demands can be met simultaneously. Given the fact that practically all the energy is contained in the two dipole modes, we can introduce the effective radiative decay rate of the nanolens as

$$\gamma_{rad}^{Lens} = \frac{|\sqrt{\gamma_{rad}^{(1)}} A_1^{(1)} + \sqrt{\gamma_{rad}^{(2)}} A_1^{(2)}|^2}{|A_1^{(1)}|^2 + |A_1^{(2)}|^2} \qquad (4)$$

and the effective volume as

$$V_{eff}^{Lens} = \frac{|E_{max,1}^{(1)}|^2 V_{eff,1}^{(1)} + |E_{max,1}^{(2)}|^2 V_{eff,1}^{(2)}}{|E_{max}|^2}, \qquad (5)$$

where E_{max} is the maximum field at the edge of sphere 2 (inset of Fig. 2). Both of these effective parameters are plotted in Fig. 3(b) as functions of gap for the optimized sphere radii a_1 and a_2 shown in Fig. 3(a). Clearly, the "best of both worlds" scenario has been achieved as the effective volume V_{eff}^{Lens} of the nanolens system remains many times smaller than the volume of larger sphere while the radiative decay rate γ_{rad}^{Lens} is nearly identical to that of the large sphere [inset of Fig. 3(b)]. In other words the effective volume of nanolens is determined by the smaller sphere acting as a resonator while the effective coupling by the larger sphere acting as an antenna—in this wider design space stronger enhancement can be attained. Further expansion of the design space with more particles should lead to even larger enhancement as had been demonstrated with larger complexes of nanoparticles.[10]

In conclusion, a simple and effective analytical model has been applied to the task of optimizing a nanolens system composed of two closely spaced metal nanoparticles. The results reveal that the system generally favors two unequal spheres, where the larger one acting as an antenna for the effective in-coupling of external fields is coupled to the smaller one that behaves as a resonator for energy confinement. The analytical approach revealing the physics behind the enhancement of fields in the nanostructures, and being fast and efficient, is well suited for optimization of complex metal nanostructures.

[1]M. Moskovits, Rev. Mod. Phys. **57**, 783 (1985).
[2]S. Nie and S. R. Emory, Science **275**, 1102 (1997).
[3]S. Pillai, K. R. Catchpole, T. Trupke, and M. A. Green, J. Appl. Phys. **101**, 093105 (2007).
[4]S. C. Lee, S. Krishna, and S. R. J. Brueck, Opt. Express **17**, 23160 (2009).
[5]J. B. Khurgin and G. Sun, Appl. Phys. Lett. **94**, 191106 (2009).
[6]G. Sun, J. B. Khurgin, and R. A. Soref, Appl. Phys. Lett. **94**, 101103 (2009).
[7]Y. Zou, P. Steinvurzel, T. Yang, and K. B. Crozier, Appl. Phys. Lett. **94**, 171107 (2009).
[8]K. Li, M. I. Stockman, and D. J. Bergman, Phys. Rev. Lett. **91**, 227402 (2003).
[9]K. Kneipp and H. Kneipp, *Surface Enhanced Raman Scattering: Physics and Applications*, Topics in Applied Physics Vol. 103, edited by K. Kneipp, M. Moskovits, and H. Kneipp (Springer, Berlin Heidelberg, 2006), p. 183.
[10]J. Kneipp, X. Li, M. Sherwood, U. Panne, H. Kneipp, M. I. Stockman, and K. Kneipp, Anal. Chem. **80**, 4247 (2008).
[11]V. M. Shalaev, *Nonlinear Optics of Random Media: Fractal Composites and Metal-Dielectric Films*, Springer Tracts in Modern Physics Vol. 158 (Springer, Berlin, Heidelberg, 2000).
[12]F. J. G. de Abajo, J. Phys. Chem. C **112**, 17983 (2008).
[13]G. Sun and J. B. Khurgin, Appl. Phys. Lett. **97**, 263110 (2010).
[14]G. Sun, J. B. Khurgin, and C. C. Yang, Appl. Phys. Lett. **95**, 171103 (2009).
[15]S. A. Maier, Opt. Express **14**, 1957 (2006).
[16]J. B. Khurgin and G. Sun, J. Opt. Soc. Am. B **26**, B83 (2009).
[17]J. B. Khurgin, G. Sun, and R. A. Soref, Appl. Phys. Lett. **94**, 071103 (2009).
[18]H. A. Haus, *Waves and Fields in Optoelectronics*, 1st ed. (Prentice-Hall, Englewood Cliffs, New Jersey, 1984).